

To be published in Landscape Ecology

DOI 10.1007/s10980-005-3166-2

Preprint version: 9/8/2005

Textural ordination based on Fourier spectral decomposition: a method to analyze and compare landscape patterns

Pierre COUTERON¹, Nicolas BARBIER² and Denis GAUTIER³

- 1- French Institute of Pondicherry (IFP), 11 Saint Louis Street, Pondicherry 605001, INDIA / Joint Research Unit (UMR) botAny and bioinforMatics of the Architecture of Plants (AMAP), Boulevard de la Lironde, TA40/PS2, 34398 Montpellier Cedex 05, FRANCE.
- 2- Research Fellow FNRS; Université Libre de Bruxelles (ULB, Free University of Brussels), Service of Botany, Systematics and Phytosociology, 50 av.F.D. Roosevelt, CP 169, B-1050 Brussels, BELGIUM.
- 3- International Centre for Research on Agronomy and Development (CIRAD), BP 1813, Bamako, MALI.

Corresponding author:

Pierre COUTERON

French Institute of Pondicherry, 11 Saint Louis Street, Pondicherry 605001, INDIA

Tel: +91 413 2334168; Fax: +91 413 2339534

pierre.couteron@ifpindia.org

Abstract

We propose an approach to texture characterization and comparison that directly uses the information of digital images of the earth surface without requesting a prior distinction of structural “patches”. Digital images are partitioned into square "windows" that define the scale of the analysis and which are submitted to the two-dimensional Fourier transform for extraction of a simplified textural characterization (in terms of coarseness) via the computation of a "radial" power spectrum. Spectra computed from many images of the same size are systematically compared by means of a principal component analysis (PCA), which provides an ordination along a limited number of coarseness vs. fineness gradients. As an illustration, we applied this approach to digitised panchromatic air photos depicting various types of land cover in a semiarid landscape of northern Cameroon. We performed “textural ordinations” at several scales by using square windows with sides ranging from 120 m to 1 km. At all scales, we found two coarseness gradients (PCA axes) based on the relative importance in the spectrum of large ($>50 \text{ km}^{-1}$), intermediate ($30\text{-}50 \text{ km}^{-1}$), small ($10\text{-}25 \text{ km}^{-1}$) and very small ($<10 \text{ km}^{-1}$) spatial frequencies. Textural ordination based on Fourier spectra provides a powerful and consistent framework to identifying prominent scales of landscape patterns and to compare scaling properties across landscapes.

Keywords: Cameroon, Central Africa, Fourier transform; multi-scale analysis; spectral analysis; Sahel; Texture feature extraction; tropical savannas; remote sensing.

Introduction

Texture, along with embedded terms such as coarseness, grain and organization, is a central concept for characterizing main spatial features of landscapes from zenithal views of the earth. Although the complexity of the concept proved hard to capture through a formal definition (Musick and Grover 1991 p.79), two main approaches, "structural" vs. "statistical" (Haralick 1979) to texture quantification have long been distinguished (see also Li and Reynolds (1995) and Turner et al. (2001)). The "structural" approach assumes that landscapes are composed of distinct primitive elements (i.e., patches, Forman and Godron 1981) that can be delineated on digital images prior to further investigation into patch characteristics, such as shape, size, spatial distribution, connectivity or diversity (Turner et al. 2001). A great deal of quantitative studies relied on such a premise, since being based on categorical maps (i.a., Cain et al. 1997; Ludwig et al. 2002). The second approach, referred to as "statistical" (Haralick 1979), directly relies on the digital values contained in a given image and aimed at characterising texture via the computation of statistical properties for neighbouring pixels (through a moving window) or for pairs of pixels located at varying distances from each others. The statistical approach to texture fits environments in which patch delineation is no easy task for either technical or conceptual reasons. This is the case of landscapes displaying continuously varying vegetation covers, or edaphic gradients that cannot be easily expressed via a set of discrete land-cover categories. For instance, arid and semiarid landscapes have been recognized as displaying progressive transitions between vegetation types and land-use units (Puech 1994).

Several statistical approaches to texture stem from the two-dimensional autocorrelation function, which provides a measure of spatial dependence between pixels (Ripley 1981 p.10). Coarse textures can be expected to determine long-range spatial dependence whilst fine textures are likely to be associated with short-range dependence (Haralick 1979). Blocked-quadrat variances and variograms are closely related to the autocorrelation function (Ver Hoef et al. 1993) and are to be seen as complementary ways of looking at the same information. An alternative standpoint is to submit the autocorrelation function to the Fourier transform (Mugglestone and Renshaw 1998) to compute a spectral density (or power spectrum). The Fourier spectrum has some interesting statistical properties (Ripley 1981 pp.79-87) and, hence, may be of easier to interpret.

Spectral analysis by Fourier transform, a well-known technique, which plays a prominent role in signal processing (Kumaresan 1993), has been scarcely used for landscape characterisation in spite of some promising prospects (Turner et al. 1990). The reason may be that spectral analysis is mostly perceived as only useful for studying genuine periodicity, a property that is not expected in most regions of the earth surface. However, spectral analysis is also an efficient way to model and approximate any signal in terms of simple cosine and sine functions that explicitly refer to spatial frequency (Keitt 2000), i.e. to the number of times a feature repeats itself within a given area. A fair approximation of a coarse texture may be expected from a limited number of periodic functions having small spatial frequencies (large wavelengths), whilst a finer texture is likely to request additional functions relating to small wavelengths. Consequently, the relative contribution to the Fourier approximation of large vs. small wavelengths can be thought of as a good expression of the relative importance of coarse vs. fine textural components in a digital image. If so, using multivariate analysis to compare many Fourier spectra, a process we shall refer to as "textural ordination", may allow a consistent investigation into textural properties of many images having the same resolution and extent (size), i.e. scale (sensu Turner et al. 2001). Furthermore, iterating the analysis over several sizes of images may provide valuable insights into the relationship between texture and scale in the landscapes under study.

The present paper aims to describe the method of textural ordination and to illustrate its potential by investigating some textural and scaling properties of a remotely sensed semiarid landscape in northern Cameroon (Central Africa). We used textural ordination to identify main coarseness vs. fineness gradients, to quickly extract images typical of a coarseness class and to map and test coarseness variation. We carried out textural ordinations for reference images ("windows") having hectometric to kilometric sizes, in order to assess the potential influence of spatial scale on ordination results.

Material and methods

Study area and field description

To illustrate the potential of textural ordination, we selected a very diversified study area, extending over 800 km² (around 14.5° North latitude and 11° West longitude in the Extreme-Northern Province of Cameroon) and encompassing most vegetation types and land uses

found in the lowlands of northern Cameroon. Climate is semiarid tropical with a four months rainy season, centered on August, and yielding average rainfall of slightly less than 700 mm year⁻¹ (L'Hôte 2000). A fossil sand dune (320 m above sea level), corresponding to a former shore of Lake Chad, intersects the study area from North-West to South-East, thereby, distinguishing a very flat plain on its North-Eastern side from a glaciais of accumulation of the Mandara Mountains located in the South (Brabant and Gaveaud 1985). Seasonal rivers, which run from the mountains and disappear into endoreic deltas when approaching the dune, have constituted alluvial fans. The northern plain is punctuated by clayey depressions, which are flooded during the rainy season.

Vegetation belongs to the Sahelian Transition Zone (White 1983) which includes several types of savannas and woodlands characterized by an association of shrubs and trees to annual grasses and forbs. Perennial grasses were scattered and of limited importance. *Guiera senegalensis* (nomenclature according to Hutchinson and Dalziel (1954)), a shrub reaching a height of 3-4 m, appeared in quasi-pure stands on the poorly evolved soils of the dune, but was associated with scattered large *Sclerocarya birrea* (up to 12 m height) on solonetz soils. *Acacia seyal*, a small tree reaching 10 m, dominated on all clayey soils liable to flooding and formed dense and nearly monospecific stands on black-cotton soils. Trees of several species (up to 15 m height) were observed in either gallery forests fringing seasonal rivers or in small groves punctuating flooding areas. Although all the human populations living in the region are from a pastoral origin (Fula, Arab Shoa, Kanuri; Seignobos 2000), their use of land resources and main activities varied across the study area. On the southern side of the dune, settlements were older and bigger and the landscape matrix was made of crops (pluvial sorghum in rotation with cotton) and fallows. On the northern side of the dune, smaller settlements were more oriented towards nomadic herding, and the landscape matrix was 'spontaneous' vegetation.

Aerial photographs and digital images

The 125 air photographs covering the study area were purchased from Afrique aéro photos Ltd. Photographs were printed panchromatic contacts at a nominal scale of 1:20000. The photographs were acquired on 11/11/1995 between 9h and 11h local time, from a flight altitude of about 2900 m above sea level (ca. 2600 m above ground level) with a camera focus of 88 mm and a film size of 240 mm (each photograph related to a square of 4.8 by 4.8 km in

the field). Centres of photographs were located 2.2 km apart from each other along W-E flight lines that were separated by 3.7 km.

The present analysis only considered the central part of each air photo, namely a square area of 5 cm side (1 km in the field), in which geometrical deformation and reflectance discrepancy are of minor importance (Kadmon and Harari-Kremer 1999). Central parts of the 125 photographs were digitised (grey-scale value in the range 0-255) to a spatial resolution of 800 dots per inch (DPI), which equate to pixels of 0.64 m in the field. Digitised data were directly submitted to spectral analysis without any prior correction of the grey level values. In particular, reflectance correction within and between images (Dymond 1992; Kadmon and Harari-Kremer 1999) was not applied because spectral analysis is generally able to make consistent textural comparisons even between photographs of heterogeneous origins (Couteron 2002). This robustness results from the fact that neither the mean nor the variance of reflectance influences the computation of the spectrum (see Eq.1 below).

Spectral analysis by two-dimensional Fourier transform

Only broad outlines of two-dimensional spectral analysis by Fourier transform are provided here, since theoretical presentations (e.g., Ripley 1981; Kumaresan 1993), as well as applications to digital images (Mugglestone and Renshaw 1998; Couteron 2002), are available in literature. For simplicity, only square images will be considered although the method applies to rectangular images as well. A digital image is here defined as an n by n array of grey-scale values in the range 0-255 expressing the panchromatic radiance of each pixel. Spectral analysis aimed at modelling such data as a weighted sum of cosine and sine waveforms of varying travelling direction and spatial frequency. For a given geographical direction, the wavenumber, p , quantifies spatial frequency and is defined as the number of times a waveform repeats itself within the image under study. Wavelength is the dimension of the square image divided by the wavenumber. Expressing p in cycles per kilometre is convenient to compare results from images of different sizes and has been adopted for the present study. However, for a given image size, s , the Fourier decomposition always relies on a discrete set of spatial wavelengths, that is: $s/1, s/2, s/3, \dots, s/p, \dots, s/p_{max}$. The highest wavenumber to be computed, p_{max} , also known as Nyquist frequency, is $n/2$ or, equivalently, $s/(2d)$ if d is the size of the pixel.

Let us consider a specific couple of wavenumbers (p,q) along the two Cartesian directions of the geographical space. Fourier coefficients $(a_{pq}$ and $b_{pq})$ are weights of cosine and sine waveforms, respectively, in the linear model of image radiance. The complete set of a_{pq} and b_{pq} coefficients ($1 \leq p \leq p_{\max}$, $1 \leq q \leq q_{\max}$) can be efficiently computed via the two-dimensional Fast Fourier Transform (FFT; Diggle 1990). The subsequent stage of analysis is to ignore phase information, whose potential contribution to texture classification is a controversial question (Tang and Stewart 2000), and to compute periodogram values as: $G_{pq} = n^{-2}(a_{pq}^2 + b_{pq}^2)$. The periodogram is, thus, proportional to the portion of the total image variance that can be accounted for by the waveform defined by (p,q) . Equivalently, in polar form, periodogram values, $I_{r\theta}$, are portions of image variance accounted for by a waveform having spatial frequency r and travelling direction θ , with $r = \sqrt{p^2 + q^2}$ and $\theta = \tan^{-1}(p/q)$.

For each r , averaging $I_{r\theta}$ values on all possible directions (θ) yields an azimuthally averaged "radial" spectrum (also called r-spectrum), $I(r)$, i.e.:

$$I(r) = (k\sigma^2)^{-1} \sum_{\theta} I_{r\theta} \quad \text{Eq.1}$$

where k is the number of periodogram values making bin r , and where σ^2 is the image variance. The radial spectrum is a convenient way to reduce the information contained in the periodogram to the sole textural properties related to coarseness and fineness ("scale" sensu Mugglestone and Renshaw 1998). This property applies because images with a coarse texture will yield a radial spectrum that is skewed towards small spatial frequencies, whereas fine-textured images will have more balanced spectra. An image, in which each pixel takes a random value independent of the value taken by any other pixel, will have the finest possible texture and a virtually flat spectrum. In the present paper, we put emphasis on the potential and usefulness of a systematic comparison of radial spectra to investigate coarseness-related landscape properties. This, of course, does not preclude considering directional information, via "angular", " Θ -spectra" (Mugglestone and Renshaw 1998; Couteron and Lejeune 2001) for the study of landscape textural properties, nor using the entire information of the periodogram. This last approach has been recognized as very efficient for discriminating textural classes (Tang and Stewart 2000) but several developments, which are beyond the scope of the present paper, are still needed to permit an explicit interpretation of the results in terms of coarseness and directionality.

Insert Figure 1 approximately here

Ordination of radial spectra

We carried out a systematic textural analysis that started by partitioning the kilometeric areas ("sub-photo") digitised from each photograph into identical square "windows" (Figure 1) at the scale for which radial spectra were computed. We used window sizes ranging from 120 m up to 1 km. For each particular window size, a general table was built in which each row was the radial spectrum of a given window, while each column contained the portions of the windows' variance explained by a given spatial frequency. Each of these tables of spectra was submitted to a principal component analysis (PCA; Manly 1994), thus we treated windows as statistical observations characterised by their spectral profile, i.e., the way in which window variance is broken down in relation to spatial frequencies. Conversely, spatial frequencies are seen as quantitative variables that are to be linearly combined to yield principal components. We used standardized PCA to avoid excessive influence of small spatial frequencies. We consistently consider only the first 25 wavenumbers so all PCAs had a constant total variance of 25, whatever the window size. Our approach differs from the method used by Ares et al. (2003) in several points. Because we computed spectra from two-dimensional image periodograms (instead of 1-D periodograms from transects), we do not perform preliminary image filtering, and we used 25 spectral values instead of a unique signal/noise ratio to compare and interpret spectra.

Statistical comparison between radial spectra

For a completely random image, we should have a flat spectrum with values following a defined statistical distribution, namely:

$$I(r) \sim (2k)^{-1} \chi_{2k}^2 \quad \text{Eq.2}$$

with an expectation of 1 and a variance of 2 (Mugglestone and Renshaw 1998). Testing against complete randomness is of limited interest since spectra found for all views of the earth of a reasonable resolution are always far above the upper confidence envelope. However, two spectra, say $I_1(r)$ and $I_2(r)$, can be compared via their ratio $R(r)=I_1(r)/I_2(r)$, which is expected to be 1 under the null hypothesis of identity between the two spectra

(confidence envelopes are built from a Fisher-Snedecor distribution, $F_{2k,2k}$). This last result is a straightforward extension to radial spectra of the principle thoroughly exposed by Diggle (1990 p.117-119) for the ratio of mean spectra from one-dimensional time series. Identity of mean radial spectra computed from two batches of m and l images, respectively, is also addressable in the same way but with increased degrees of freedom (envelopes are built from $F_{2km,2kl}$). The log-ratio, i.e. $\log(R)$, is generally used for plotting (Diggle 1990).

Results

Textural ordination using a small-sized window

We first sampled the set of 125 aerial photographs using windows of 180 m (250 pixels) and radial spectra were computed for each of the 4500 resulting windows (i.e., 36 per sub-photo). The PCA of the table of spectra yielded a prominent first axis (about 55% of total variance; Figure 2a) along with a less important, yet significant, second axis (eigenvalue of 3, i.e., about 15.6% of total variance). Subsequent axes were of low interest since none of the relating eigenvalues was above 1. Small spatial frequencies ($<20 \text{ km}^{-1}$, that is, wavelengths above 45 m, coarse textures) and large spatial frequencies ($>50 \text{ km}^{-1}$, i.e., wavelengths of less than 20 m, fine texture) had strong loadings on the first axis (Figure 2b) while displaying opposite correlations (Figure 2c). Intermediate frequencies ($20\text{-}50 \text{ km}^{-1}$) had high loadings on axis 2 in contrast with small frequencies.

Insert Figure 2 approximately here

Plotting windows within PCA axes (Figure 2d) yielded a cloud of points with no obvious discontinuity, indicating that coarseness variation related more to continuous gradients than to separate types. We based a first interpretation on the automatic identification of windows with extreme coarseness properties, which correspond to locations far away from the origin of PCA axes. In a given angular sector of the PCA plane, windows located farthest from the origin are those that typify a class of spatial patterns characterised by the importance of the range of spatial frequencies corresponding to the angular sector under consideration. For example, focusing on the angular sector $[\pi/8, 3\pi/8]$ as in Figure 2d, enabled the selection of windows for which spatial frequencies in the range $17\text{-}28 \text{ km}^{-1}$ accounted for a large share of window variance (Figure 2b). This does not automatically mean that the spectra peaked for

this range of frequencies, but that they distinguish themselves from other spectra by a higher share of variance accounted for by the aforementioned frequency range. For illustration purpose, we used five angular sectors (see Figure 3 for their definition) and, thus, five coarseness classes, while automatically extracting in each sector the 12 windows most apart from axes' origin. Among them, two windows were subjectively selected for display in Figure 3 as to illustrate textures found within each of the five classes. Mean radial spectra of the five classes are plotted in Figure 4.

The first class (C1; Figure 3a,b) related to fine-grained patterns, which were characterized by balanced, rather flat, spectra (Figure 4a), and for which spatial frequencies above 60 km^{-1} (wavelengths under 20 m) explained a substantial share of windows' variance. Some of these patterns (Figure 3a) corresponded to savanna vegetation, with a rather homogeneous spatial distribution of trees and/or clumps of trees (dark grey dots) on a white or light-grey background expressing bare soil or grassy vegetation of low biomass. Other fine-grained patterns (Figure 3b) were made of the distribution of canopy gaps that punctuated the dense monospecific woodlands of *Acacia seyal* found on black cotton soils. We note that results of the textural analysis would not have been changed by a reversal of the grey-level scale (i.e., bare soil turning dark-grey and vegetation becoming light-grey). Indeed, neither mean nor variance of the windows' gray levels is taken into account by the Fourier decomposition. This explains why connected woody cover with scattered gaps had similar coarseness attributes to savanna vegetation with scattered trees. However, if deemed necessary, it would be possible to discriminate these two vegetation types from the shape of the histogram of their gray-levels values.

Insert Figure 3 approximately here

The second coarseness class (C2; Figure 3c,d) was characterized by spatial frequencies in the range $22\text{-}50 \text{ km}^{-1}$ (Figure 4a) and featured dense clumps of woody vegetation with a diameter ranging from 10 to 35 m (Figure 3d). Such a physiognomy was observed in floodplains with highly clayey soils. Another kind of pattern, looking somewhat like the reverse of the previous one (Figure 3c), was made of spots of bare soils punctuating vegetation cover. This pattern has been reported as being a frequent feature on degrading solonetz soils (Brabant and Gaveaud 1985). Patterns with spots of a larger size (dominant spatial frequencies in the range $15\text{-}20 \text{ km}^{-1}$, Figure 3e and Figure 4a) were also found in a

third coarseness class (C3), along with patterns of coalescing bare areas originating from heavy human disturbance in or around small villages (Figure 3f).

The fourth coarseness class (C4; Figure 3g,h) contained patterns that were clearly macro-heterogeneous at the scale of the window size. Such patterns, which were mostly observed in cultivated and/or man-disturbed areas, yielded radial spectra (Figure 4b) that were markedly skewed towards small spatial frequencies ($<12 \text{ km}^{-1}$). For instance, a strong dominance of the first wavenumber (6 km^{-1}) denoted situations for which the window was partitioned between a vegetated and a bare part. The last coarseness class (C5; Figure 3i,j) was characterized by the concomitant presence of macro-heterogeneity and fine-grained features, including ecotones between woodland and grassland (Figure 3i) and gallery forests if they were fringed by denuded foot-slopes (Figure 3j). All the windows belonging to class C5 had negative coordinates along the second PCA axis (Figure 2b) due to a weak contribution of intermediate spatial frequencies (Figure 4b), while having intermediate coordinates along axis 1.

Insert Figure 4 approximately here#

Mapping textural variation

PCA scores of windows can also be used to map coarseness variation (Figure 1) while avoiding the subjectivity that would be attached to any attempt of visual delineation. This is illustrated from a particular sub-photo of 1 km^2 , which displayed contrasted textural aspects (Figure 5a). Negative scores on axis 1 clearly delineated the fine-grained area on the sand dune (lower-left half; Figure 5b), while the part of coarser texture, near the upper-right corner, stood out due to intermediate values on axis 2 (Figure 5c). Interestingly, the transition zone that runs along the diagonal of the 1 km sub-photo was also identified as having an intermediate, yet specific, texture (see also the spectra in Figure 5d). We note that a more precise delineation of the three distinct textural areas could have been easily achieved by computing spectra and PCA scores for sliding windows of 180 m instead of non-overlapping ones.

Insert Figure 5 approximately here#

Influence of window size

We compared results of the coarseness ordination for various window sizes ranging from 120 m to 1 km. For all sizes, there were always two prominent PCA axes (result not presented), indicating the existence of two independent coarseness gradients, and these two axes accounted for a steady share of the total variance of the table of spectra (about 70%). Subsequent axes were negligible, with eigenvalues always below 1. Axis 1 was clearly prominent for the smaller window size (55% of total variance vs. 15% for axis 2), but the gap between both axes narrowed with increasing window size (38% vs. 31% for windows of 500 m), before widening again (56% vs. 16% for windows of 1 km).

Insert Figure 6 approximately here#

Whatever the window size, spatial frequencies displayed more or less the same patterns of contribution to PCA axes, a fact that can be made clear by plotting PCA loadings as a function of spatial frequencies for window sizes of 180 m, 500 m and 1 km (Figure 6). The first pattern (Figure 6a) illustrates a contrast between small frequencies in the range 5-25 km^{-1} and large frequencies above 50 km^{-1} . This contrast was apparent on PCA axis 1 when small windows were used (see Figure 2b), but was also clearly detectable with windows of 500 m and 1,000 m (but on PCA axis 2 for 500 m windows). For large windows, frequencies above 50 km^{-1} , though not explicitly considered by the PCA, still exerted an influence on the analysis because, whatever the window size, radial spectra have been re-scaled via a division by window variance (Eq.1) and not by the portion of variance related to the first 25 wavenumbers. The second pattern, which appeared on PCA axis 1 for 500 m windows and on PCA axes 2 for the other window sizes, contrasts frequencies of 30-50 km^{-1} to frequencies under 10 km^{-1} (Figure 6b). It was most apparent when using large windows though also slightly perceptible for the 180 m windows, which gave nevertheless no information on frequencies less than 6 km^{-1} .

It was interesting to note, on the basis of kilometric windows, that the smallest frequencies (1-2 km^{-1}) were poorly correlated with the plane defined by the two main PCA axes (Pearson's $r < 0.55$ compared to $r > 0.85$ for frequencies above 4 km^{-1}). This meant that macro-heterogeneity was no longer important at kilometric scale, which is relevant for investigating coarse-grained patterns characterized by spatial frequencies in the range 4-15

km⁻¹. The PCA carried out on spectra of 1 km windows revealed that these patterns related either to imprints of human activities, such as mosaics of crops, hamlets and networks of pastoral trails (extended versions of Figure 3f,g,h) or to geomorphologic features, such as periodic depressions in the sand dune or alluvial fans (Figure 7a). Man-induced patterns corresponded mostly to spatial frequencies of 10-15 km⁻¹ while geomorphologic features were characterized by dominant spatial frequencies in the range 4-5 km⁻¹ and demanded kilometric scale windows for being identified as a specific texture class. For alluvial fans, the characteristic aspect resulted from the presence of dense vegetation along river channels or oxbows, whereas former river banks, with clayey soils, only bore a sparse scrub.

Testing coarseness discrepancies

One may wish to know whether an identified coarseness discrepancy between two areas is to be considered as statistically significant. For instance, we found some kilometric-sub-photos of alluvial fans (as on Figure 7a) which were heavily settled whereas others were without any notable human impact. On both photographs, the overall network of former river channels and oxbows expresses itself at comparable scale. But, to the naked eye, the areas experiencing a light human pressure were characterized by a far higher density of the small black spots that correspond to trees and large shrubs in the field (Figure 7a). The question is, are such differences revealed by significant differences between spectra? The question is worth considering because it would also allow us to characterize human-induced change, if multi-temporal air coverage were to be analyzed.

Insert Figure 7 approximately here#

Plotting the positions of 180 m windows in the corresponding PCA plane enabled us to detect that windows depicting the heavily utilized situation were located farther from the origin of PCA axes than windows relating to the lightly used area (Figure 7c). In the PCA plot, the two groups of points barely overlap and proved significantly shifted along axis 1 ($P < 10^{-2}$) and axis 2 ($P < 10^{-3}$) in the light of the rank-based Wilcoxon's test (Sokal and Rohlf 1995). This was due to the fact that, in accordance with visual impression, windows belonging to the less disturbed area have a greater share of their variance explained by very large spatial frequencies ($>70 \text{ km}^{-1}$) along with a lower share accounted for by spatial frequencies in the range of ca. 20 km^{-1} . This was also clearly apparent when plotting the log-ratio of the two

mean spectra (Figure 7d), which was successively below and above confidence envelopes for spatial frequencies around 20 km^{-1} and above 60 km^{-1} , respectively.

Discussion

Performing a multivariate analysis of the table of radial spectra to summarize the results of a two-dimensional Fourier decomposition (Figure 1) is a very simple, yet new, powerful and somewhat generic idea. Though the approach was considered in the present paper with respect to air photographs and for hectometric to kilometeric scales, it may be potentially relevant for analyzing most kinds of numerical images describing the earth surface. This method is likely to yield results that are fully interpretable in terms of coarseness with no confusion with other textural properties. One other interest is that there is no a priori hypothesis about the structure of the image under study, since no specific shape of the spectrum is postulated. Zenithal images drawn from our study site displayed, indeed, spectra of varying shape, some of them being linear and agreeing with a fractal structure (Keitt 2000), at least for the considered range of spatial frequencies, whereas others were found curvilinear, due to the predominance of particular ranges of spatial frequencies. Of course, images displaying strongly periodic banded or spotted patterns (see Tongway et al. 2001 for a detailed account), which were not present in our study area, may have been efficiently and consistently characterized (Couteron 2002). PCA results not only distinguished spectra having different shapes, but also revealed subtle variations among spectra of similar shape. Thus, very diverse spatial patterns can be consistently compared and classified within the same framework of analysis, and our method of coarseness (texture) ordination can be useful at different steps of an investigation into landscape properties.

The present paper proposes an approach to texture that is solely based on the radial spectrum that is, on a limited part of the information conveyed by the two-dimensional Fourier periodogram. Ordination using radial spectra is, nevertheless, due to yield at least one or two independent coarseness gradients, depending on the nature of the landscape features under study. (For the canopy of a tropical primary rainforest, most of coarseness variation appeared summarized by a single PCA axis; Couteron et al. in press). Hence, from a panchromatic image, one or two independent coarseness layers, i.e. "textural transforms" (Haralick 1979), can be produced. Valuable and complementary textural information, to be expressed as additional layers, can also be expected from directional features via analyses based on angular spectra (see Mugglestone and Renshaw 1998 or Couteron and Lejeune 2001 for definition and

use). This is to say that results of ordination-based textural transforms should not only be considered per se, but would be most useful in the framework of a geographic information system by being overlaid with other information layers either image-based or not.

Strictly speaking, results of our texture ordination depend upon the size of the window at the scale of which Fourier decomposition is carried out. Using a relatively small window size allows a precise identification and classification of fine-grained patterns, repeating themselves more than 3-4 times within the window, while larger structures, i.e. macro-heterogeneity at the window scale, mostly influence the portion of variance attached to the smallest wavenumber. Increasing window size may enable a better discrimination between some of these broader patterns at the risk of a less precise classification of finer patterns. (Wavenumbers above 20-25 are usually too inter-correlated to help distinguish among patterns in the PCA results.) In practice, however, main correlations between spatial frequencies and PCA axes may be quite stable for a wide range of window sizes. This proved true in our study area where PCA axes always expressed a double contrast between frequencies in the range $5\text{-}25\text{ km}^{-1}$ vs. $>50\text{ km}^{-1}$ and $30\text{-}50\text{ km}^{-1}$ vs. $<10\text{ km}^{-1}$, which can be considered as a prominent feature of the landscape under study. Indeed, intermediate to fine-textured patterns ($>30\text{ km}^{-1}$) mostly related to natural vegetation, very coarse patterns ($<10\text{ km}^{-1}$) were mainly linked to geomorphologic structures and coarse patterns ($10\text{-}25\text{ km}^{-1}$) often marked places experiencing a high level of human disturbance. Another interesting result was that patterns with a frequency under 4 km^{-1} proved of limited importance. Thus, in the studied region, there seems to be no obvious reason to use windows with a side of, say 1.5 km, instead of 1 km, although there was a need of 1 km windows to properly depict structures like alluvial fans. Having texture ordination results sometimes differing with window size and thus with scale, does not mean that any scale is automatically of equivalent interest to understanding main properties of a particular landscape (Turner et al. 2001 p.38). It is, thus, important to have a consistent framework for identifying which ranges of scale are of prominent interest with respect to a particular type of landscape, to compare scaling rules across landscape types, and, ultimately, to gain insights on scales of interaction between patterns and processes.

Acknowledgements

We thank the Lamido of Petté for his help and all the inhabitants of Petté and Fadaré lamidats for their warm welcome. Field investigations for this study have been carried out while the

first author of this paper was positioned in Montpellier, France, in the Department for Tropical and Rural Forestry (FRT) of the French National School for Forestry, Land and Water Management (ENGREF), and while the third author from CIRAD was hosted in Maroua, Northern Cameroon, by the forestry program of the Agricultural Research Institute for Development (IRAD) of the United Republic of Cameroon. We are indebted to J. Ludwig (Coordinating Editor) and to two anonymous referees for valuable comments on this paper.

References

- Ares J.O., Bertiller M.B. and Bisigato A. 2003. Estimates of dryland degradation with Fourier signatures in low-altitude monochromatic images with high spatial resolution. *Landscape Ecology* 18: 51-63.
- Brabant P. and Gavaud M. 1985. Les sols et les ressources en terres du Nord-Cameroun (Provinces du Nord et de l'Extrême-Nord). Cartes à 1 : 500 000. Collection notice explicative n°103. ORSTOM, Paris.
- Cain D.H., Riitters K. and Orvis K. 1997. A multi-scale analysis of landscape statistics. *Landscape Ecology* 12: 199-212.
- Couteron P. 2002. Quantifying change in patterned semiarid vegetation by Fourier analysis of digitised aerial photographs. *International Journal of Remote Sensing*. 23: 3407-3425.
- Couteron P. and Lejeune O. 2001. Periodic spotted patterns in semiarid vegetation explained by a propagation-inhibition model. *Journal of Ecology* 89: 616-628.
- Couteron P., Pélissier R., Nicolini E. and Paget D. 2005. Predicting tropical forest stand structure parameters from Fourier transform of very high-resolution remotely sensed canopy images. *Journal of Applied Ecology*, in press
- Diggle P.J. 1990. Time series. A biostatistical introduction., 4th edition. Oxford University Press, Oxford, UK.
- Dymond J.R. 1992. Nonparametric modeling of radiance in hill country for digital classification of aerial photographs. *Remote Sensing of Environment* 39:95-102.
- Forman R.T.T. and Godron M. 1981. Patches and structural components for a landscape ecology. *BioScience*.31: 733-740.
- Haralick R.M. 1979. Statistical and structural approaches to texture. *Proceedings of the IEEE* 67: 786-804.
- Hutchinson J. and Dalziel J.M. 1973. Flora of Tropical West Africa., 2nd edition. Crown Agents, London.

- Kadmon R. and Harari-Kremer R. 1999. Studying long-term vegetation dynamics using digital processing of historical aerial photographs. *Remote Sensing of Environment* 68: 164-176.
- Keitt T.H. 2000. Spectral representation of neutral landscapes. *Landscape Ecology* 15: 479-493.
- Kumaresan R. 1993. Spectral analysis. *In* Mitra S.K. and Kaiser J.F. (eds), *Handbook for digital signal processing*, pp. 1143-1169. John Wiley & Sons, New-York, USA.
- L'Hôte Y. 2000. Climatologie. *In* Seignobos C. and Iyébi-Mandjek O. (eds), *Atlas de la Province Extrême-Nord Cameroun*, pp.17-19. IRD, Paris, France.
- Li H. and Reynolds J.F. 1995. On definition and quantification of heterogeneity. *Oikos*. 73: 280-284.
- Ludwig J.A., Eager R.W., Bastin G.N., Chewings V.H. and Liedloff A.C. 2002. A leakiness index for assessing landscape function using remote sensing. *Landscape Ecology* 17: 157-171.
- Manly B.F.J. 1994. *Multivariate statistical methods. A primer*. Chapman & Hall, London.
- Mugglestone M.A. and Renshaw E. 1998. Detection of geological lineations on aerial photographs using two-dimensional spectral analysis. *Computers & Geosciences* 24: 771-784.
- Musick H.B. and Grover H.D. 1991. Image textural measures as indices of landscape pattern. *In* Turner M.G. and Gardner R.H. (eds), *Quantitative methods in landscape ecology*, pp. 77-103. Springer-Verlag, New-York.
- Puech C. 1994. Thresholds of homogeneity in targets in the landscape. Relationship with remote sensing. *International Journal of Remote Sensing* 15: 2421-2435.
- Ripley B.D. 1981. *Spatial statistics*. John Wiley & Sons, New-york.
- Seignobos C. 2000. Répartition et densité de la population. *In* Seignobos C. and Iyébi-Mandjek O. (eds), *Atlas de la Province Extrême-Nord Cameroun*, pp.61-63. IRD, Paris.
- Sokal R.R. and Rohlf F.J. 1995. *Biometry: the principles and practice of statistics in biological research.*, 3rd edition. Freeman, San Francisco.
- Tang X. and Stewart W.K. 2000. Optical and sonar image classification: Wavelet packet transform vs Fourier transform. *Computer vision and image understanding* 79: 25-46.
- Tongway D.J., Valentin C. and Seghieri J. 2001. *Banded vegetation patterning in arid and semiarid environments. Ecological processes and consequences for management*. Springer, New-York.
- Turner M.G., Gardner R.H. and O'Neill R.V. 2001. *Landscape ecology in theory and practice. Pattern and process*. Springer-Verlag, New-York.

Turner S. J., O'Neill R.V., Conley W., Conley M.R. and Humphries H.C. 1991. Pattern and scale: statistics for landscape ecology. *In* Turner M.G. and Gardner R.H. (eds), Quantitative methods in landscape ecology, pp.17-47. Springer-Verlag, New-York.

Ver Hoef J.M., Cressie N.A.C. and Glenn-Levin D.C. 1993. Spatial models for spatial statistics: some unification. *Journal of Vegetation Science* 4: 441-452.

White F. 1983. The vegetation of Africa. A descriptive memoir to accompany the UNESCO/AEFTAT/UNSO vegetation map. UNESCO/AETFAT/UNSO, Paris

Figure captions

Figure 1: Flow diagram describing the successive stages involved in textural ordination. The flow of computations and analyses can be carried out for various window sizes, i.e., at varying scales.

Figure 2. Main results of the Principal Component Analysis (PCA) for a window size of 180 m. a) Importance of the first eight eigenvalues. b) Loadings for PCA axis 1 (solid line) and axis 2 (interrupted line) as a function of spatial frequencies (km^{-1}). Loadings have been re-scaled via a multiplication by the square root of axes' eigenvalues. c) Correlation between spatial frequencies and PCA axes (some of the frequency classes above 50 km^{-1} are omitted for legibility). d) Cloud of windows' positions in the plane defined by axes 1 and 2. The contour line delineates the part of the cloud encompassing 95% of the points; only those windows located within the angular sector $[\pi/8, 3\pi/8]$ are explicitly displayed as points.

Figure 3. Examples of 180 m windows typifying five main coarseness classes observed in the study area. The five classes have been defined from angular sectors (central orientations denoted by an arrow) in the reduced spectral plane provided by PCA and presented in Figure 2 (the shaded shape delineates the cloud of windows positions as in Figure 2d), i.e., $C1 = [\pi, 5\pi/4]$, $C2 = [\pi/4, 3\pi/4]$, $C3 = [0, \pi/4]$, $C4 = [-\pi/4, 0]$; $C5 = [-3\pi/4, -\pi/2]$. Each angular sector is characterized by a specific shape of the Fourier spectrum (see Figure 4) due to the relative dominance of a specific range of spatial frequencies (see Figure 2c). For each angular sector, those 12 windows having the farthest location from the origin of PCA axes (i.e., being most typical of a coarseness class) were automatically extracted. Among them, two windows were visually selected to illustrate the class.

Figure 4. Mean spectra for the five texture classes illustrated in Figure 3 (180 m windows). a) Mean spectra for classes C1 (solid line), C2 (dotted line) and C3 (dashed line). b) Mean spectra for classes C4 (solid line) and C5 (dashed line). For each type, the mean is computed from the 40 windows identified from their PCA scores as most typical of the texture class.

Figure 5. Mapping texture variation within a particular sub-photo of 1 km. a) Overall aspect. b) Map of scores along the first PCA axis for windows of 180 m. c) Map of scores along the second axis. The scale along both axes is consistent with Figure 2d. d) Mean spectra for the

three areas of distinct texture: fine-grained area (dotted line), coarse-grained area (dashed line) and transition zone (solid line).

Figure 6. Contribution of spatial frequencies to PCA axes for three distinct sizes of windows. Results relating to windows of 1 km, 500 m and 180 m are denoted by solid, dashed and dotted lines, respectively. To ease comparison, PCA loadings have been re-scaled via a multiplication by the square root of axes' eigenvalues. a) Pattern opposing small ($10\text{-}25\text{ km}^{-1}$) and large frequencies ($> 50\text{ km}^{-1}$), apparent on PCA axis 1 for 180 m and 1 km windows and on PCA axis 2 for 500 m windows. b) Pattern opposing very small ($< 10\text{ km}^{-1}$) and intermediate frequencies (ca. 40 km^{-1}) on PCA axis 2 for 180 m and 1 km windows and on PCA axis 1 for 500 m windows.

Figure 7. Testing the statistical significance of a spectral discrepancy. An illustration based on two 1 km sub-photos located in two distinct alluvial fans. a) Sub-photo with a low human pressure. b) Sub-photo with a heavy human pressure. c) Position of 180 m windows along the first two PCA axes (scores relate to Figure 2d); crosses and dots denote heavily and lightly utilised situations, respectively. d) Ratio of the mean spectra (mean spectrum of the lightly used situation in the denominator), with 5% bilateral confidence envelopes (dotted lines).

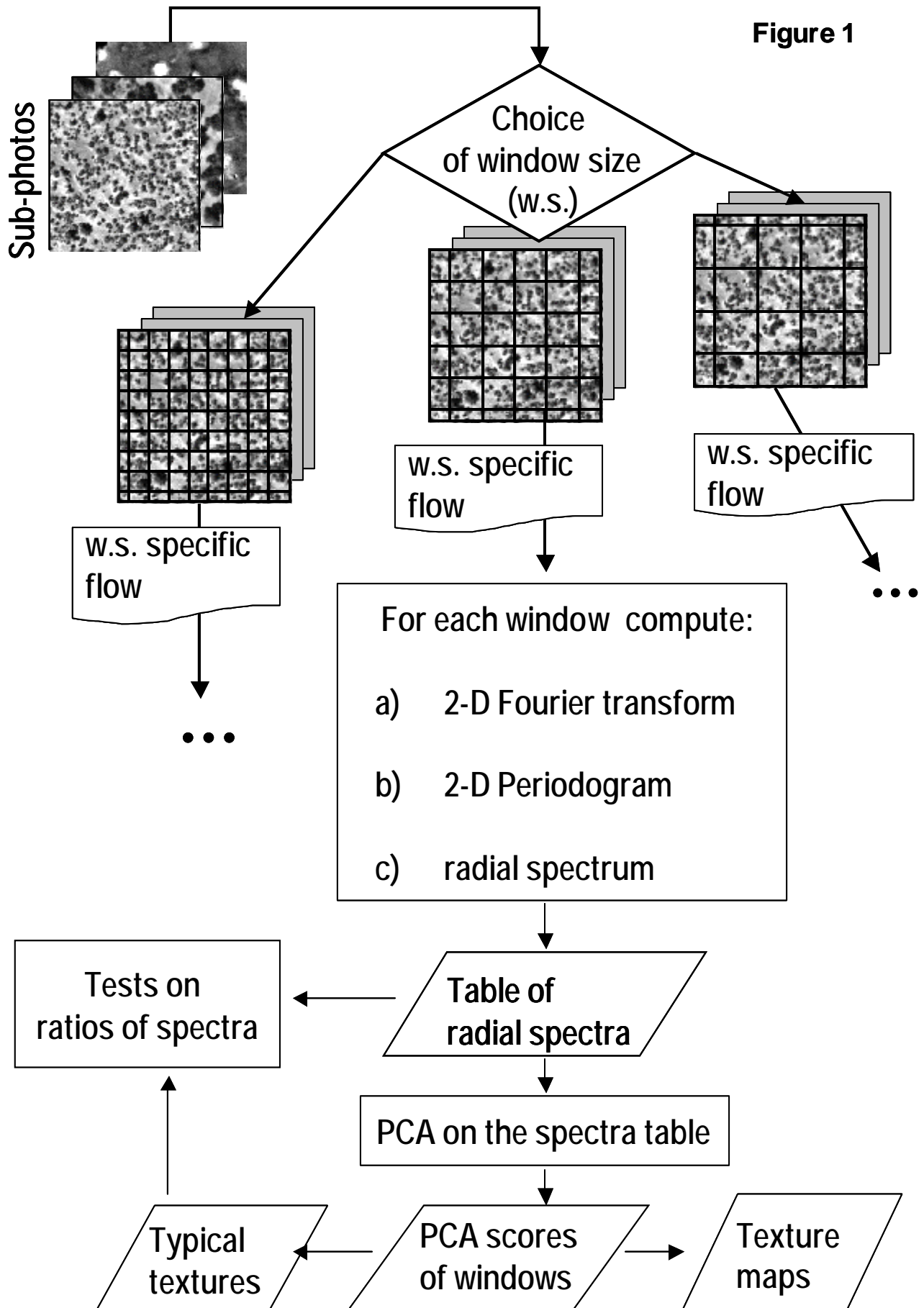


Figure 2

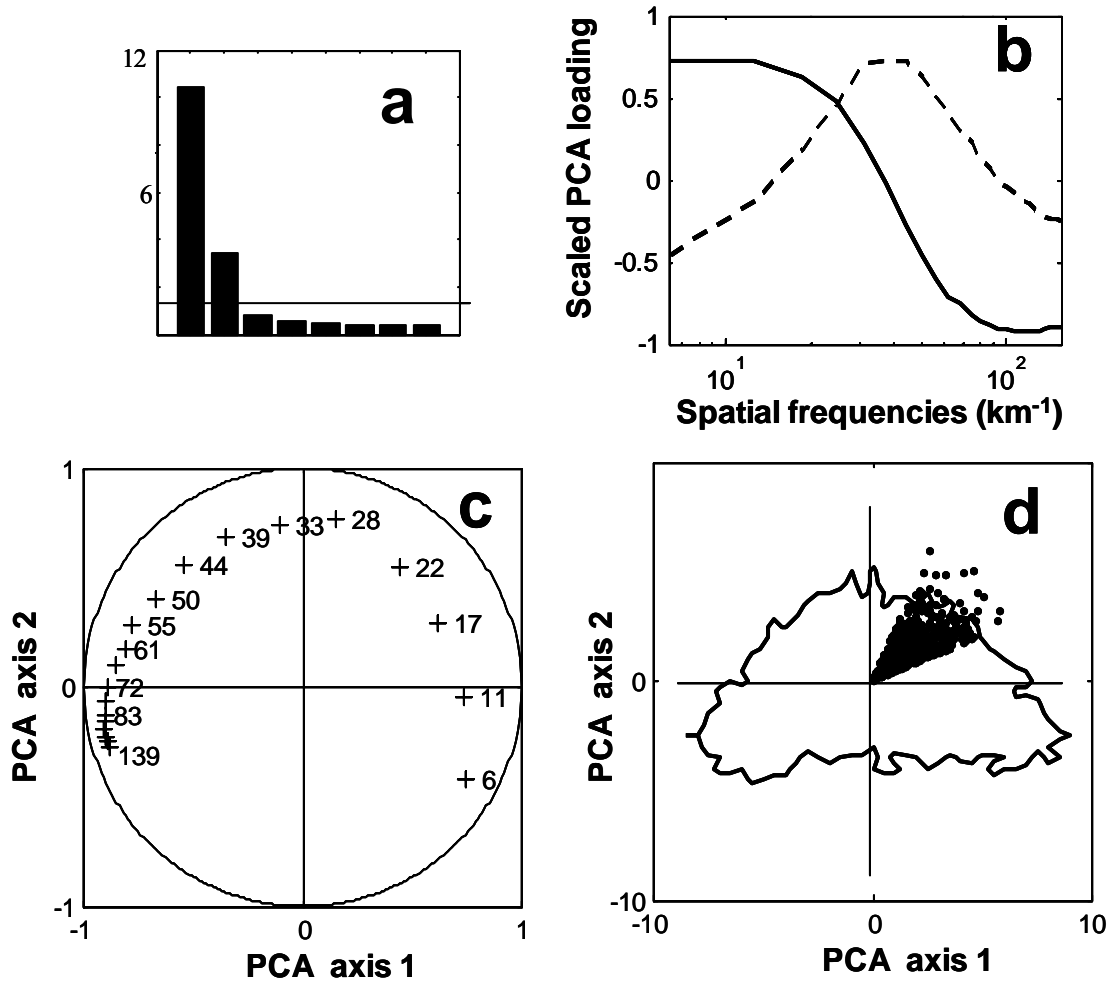


Figure 3

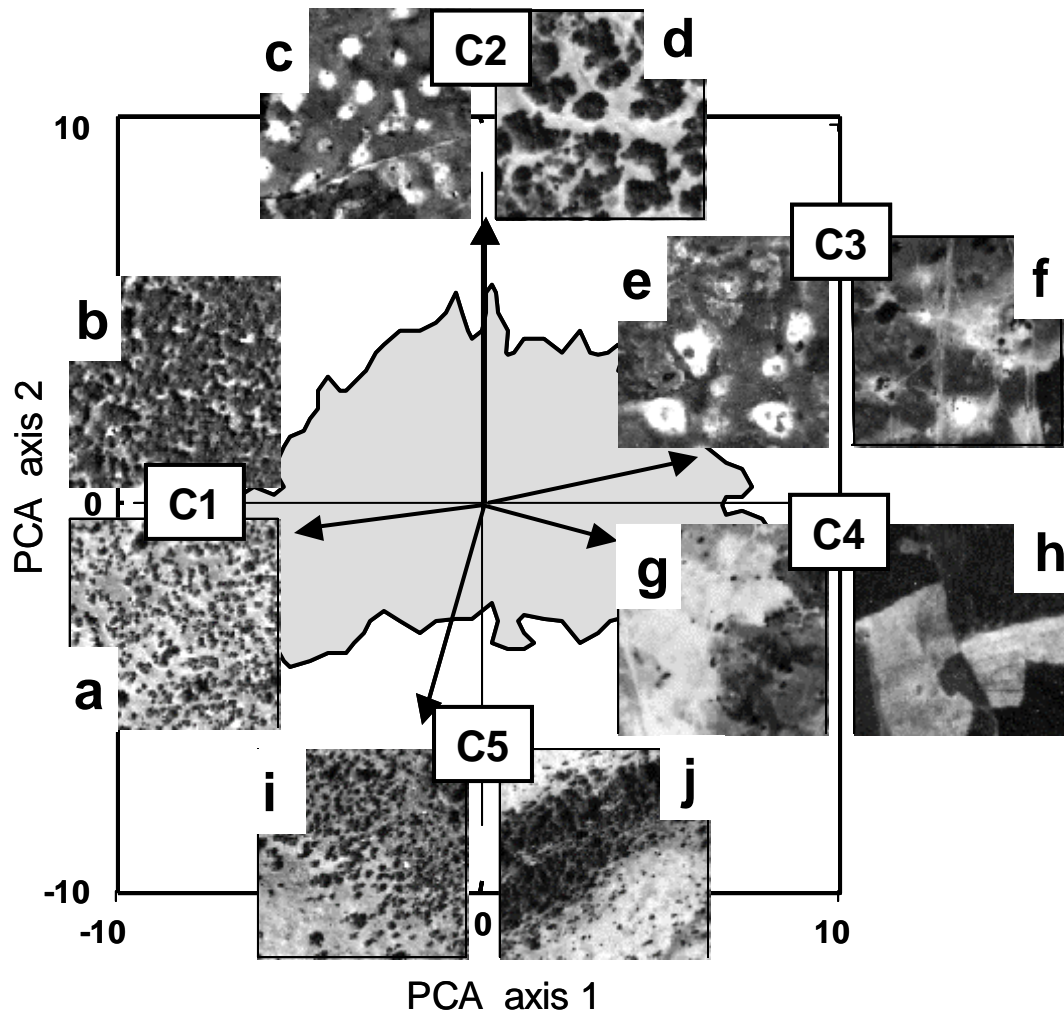


Figure 4

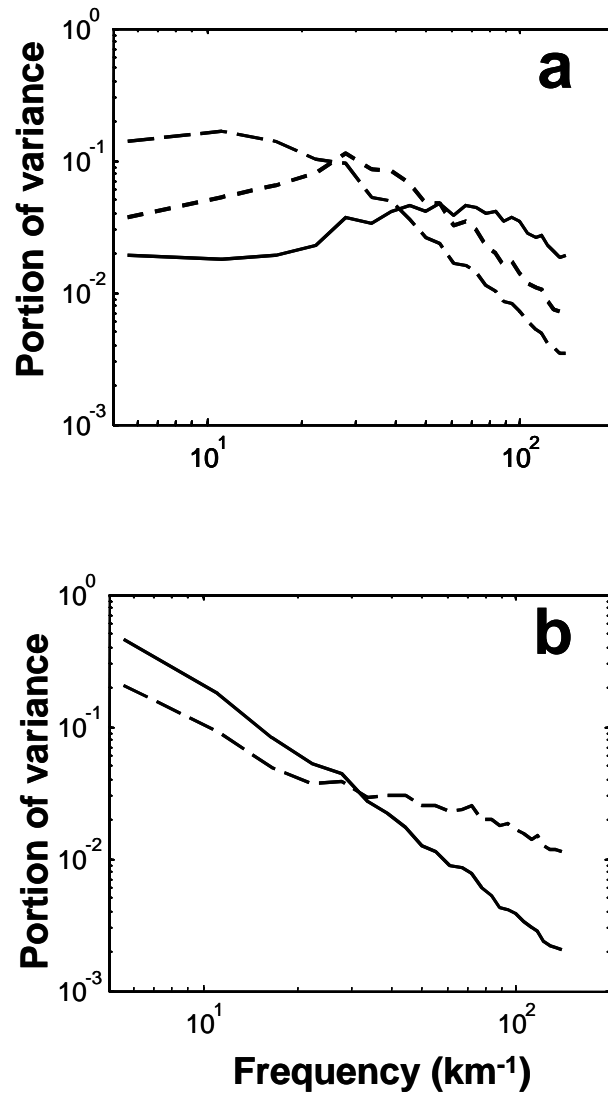


Figure 5

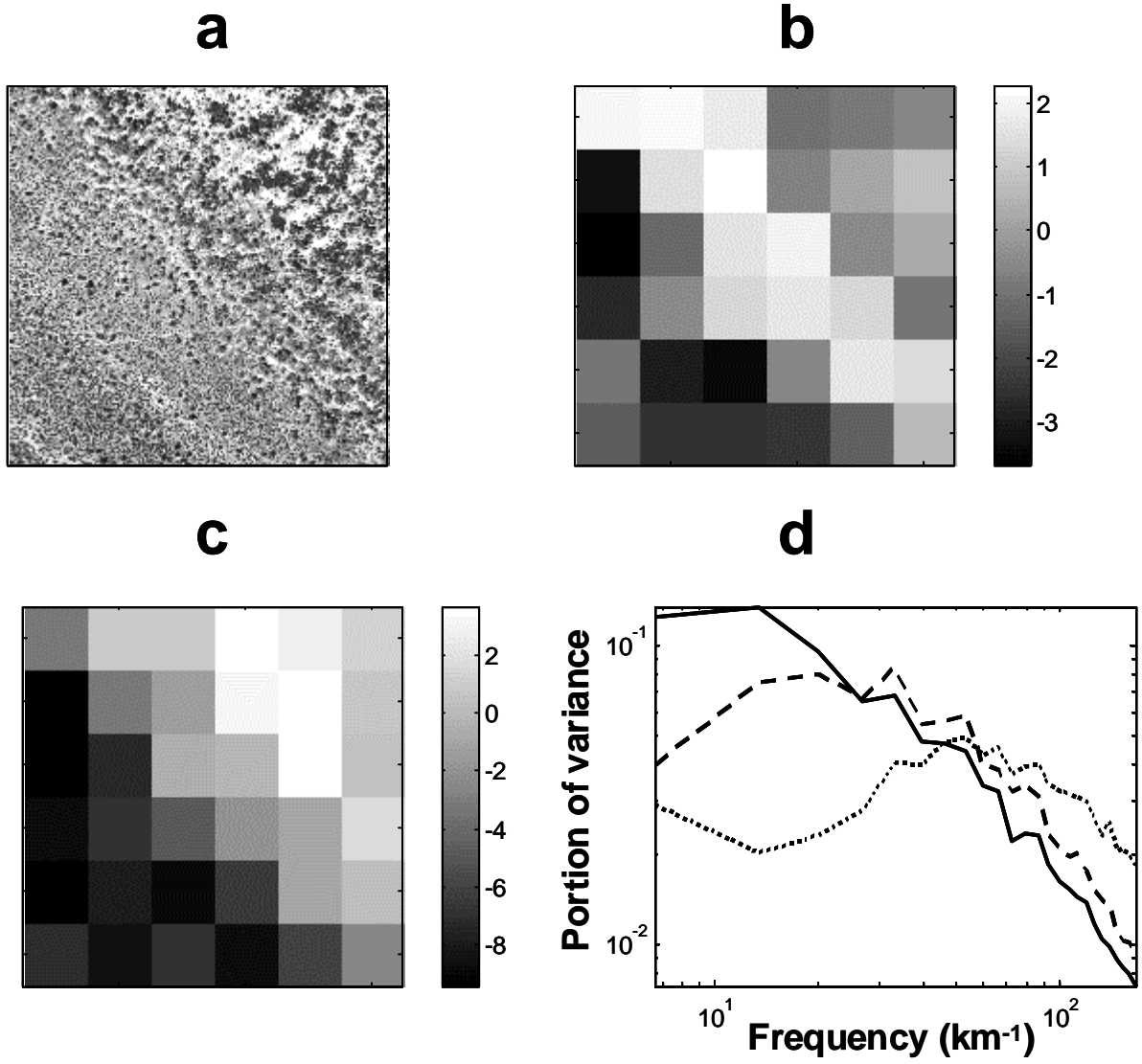


Figure 6

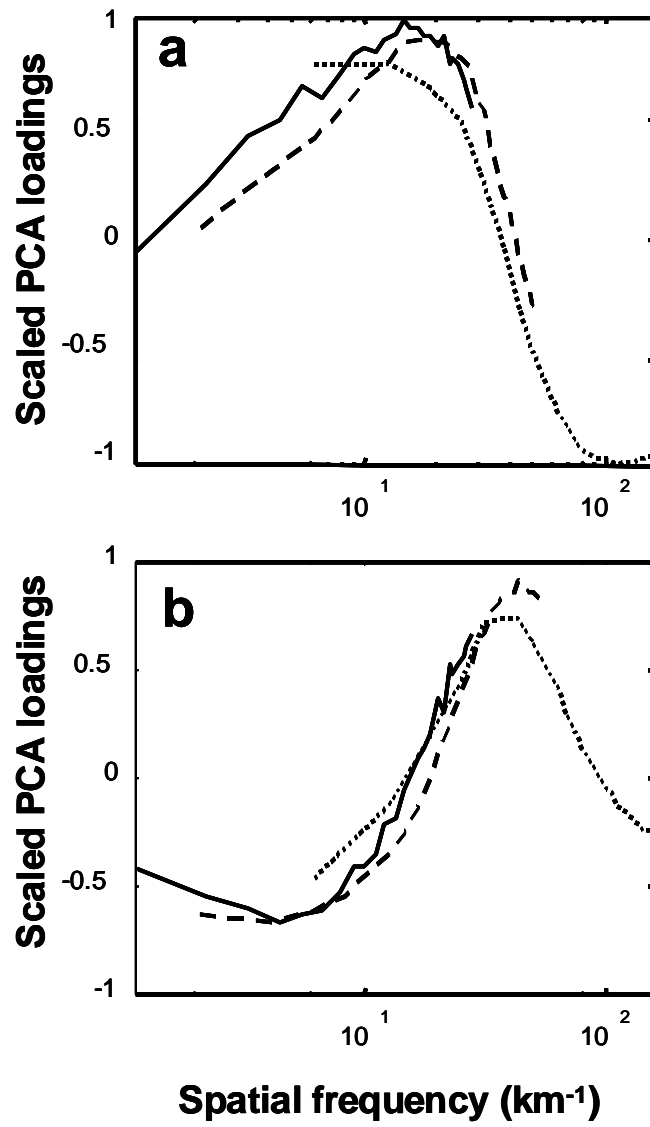


Figure 7

